Pharmaceutical Research, Vol. 24, No. 4, April 2007 (© 2007)
DOI: 10.1007/s11095-006-9212-1

Featured Article

Differentiation Restricted Endocytosis of Cell Penetrating Peptides in MDCK Cells Corresponds with Activities of Rho-GTPases

Christina Foerg,[1] Urs Ziegler,[2] Jimena Fernandez-Carneado,[3] Ernest Giralt,[3,4] and Hans P. Merkle[1,5,6]

Received October 15, 2006; accepted December 8, 2006; published online March 3, 2007

Purpose. Cellular entry of biomacromolecules is restricted by the barrier function of cell membranes. Tethering such molecules to cell penetrating peptides (CPPs) that can translocate cell membranes has opened new horizons in biomedical research. Here, we investigate the cellular internalization of hCT(9-32)-br, a human calcitonin derived branched CPP, and SAP, a γ-zein related sequence.
Methods. Internalization of fluorescence labelled CPPs was performed with both proliferating and confluent MDCK cells by means of confocal laser scanning microscopy (CLSM) and fluorescence activated cell sorting (FACS) using appropriate controls. Internalization was further elaborated in an inflammatory, IFN-γ/TNF-α induced confluent MDCK model mimicking inflammatory epithelial pathologies. Activities of active form Rho-GTPases (Rho-A and Rac-1) in proliferating and confluent MDCK cells were monitored by pull-down assay and Western blot analysis.
Results. We observed marked endocytic uptake of the peptides into proliferating MDCK by a process suggesting both lipid rafts and clathrin-coated pits. In confluent MDCK, however, we noted a massive but compound-unspecific slow-down of endocytosis. This corresponded with a down-regulation of endocytosis by Rho-GTPases, previously identified to be intimately involved in endocytic traffic. In fact, we found endocytic internalization to relate with active Rho-A; vice versa, MDCK cell density, degree of cellular differentiation and endocytic slow-down were found to relate with active Rac-1. To our knowledge, this is the first study to cast light on the previously observed differentiation restricted internalization of CPPs into epithelial cell models. In the inflammatory IFN-γ/TNF-α induced confluent MDCK model mimicking inflammatory epithelial pathologies, CPP internalization was enhanced in a cytokine concentration-dependent way resulting in maximum enhancement rates of up to 90%. We suggest a cytokine induced redistribution of lipid rafts in confluent MDCK to cause this enhancement.
Conclusion. Our findings emphasize the significance of differentiated cell models in the study of CPP internalization and point towards inflammatory epithelial pathologies as potential niche for the application of CPPs for cellular delivery.

KEY WORDS: cell penetrating peptides; cellular internalization; endocytosis; MDCK; Rho-GTPases.

INTRODUCTION

The plasma membrane of mammalian cells widely restricts the passage of large, charged and hydrophilic compounds into cells, preventing most peptide, protein and nucleic acid biopharmaceuticals to reach intracellular targets, and frequently results in low or zero biological efficacy. Cell penetrating peptides (CPPs) constitute a collection of various families of short peptide sequences that have been shown to translocate across the plasma membrane via different mechanisms. The prospects of chemical ligations or physical assemblies between CPPs and therapeutic cargoes has, therefore, attracted

This work was supported by the Commission of the European Union (EU project on Quality of Life and Management of Living Resources, Project No. QLK2-CT-2001-01451.

[1] Institute of Pharmaceutical Sciences, ETH Zurich, Zurich, Switzerland.
[2] Institute of Anatomy, University of Zurich, Zurich, Switzerland.
[3] Institut de Recerca Biomèdica de Barcelona, Parc Científic de Barcelona, Barcelona, Spain.
[4] Departament de Química Orgànica, Universitat de Barcelona, Barcelona, Spain.
[5] Department of Chemistry and Applied Biosciences, Institute of Pharmaceutical Sciences, ETH Zurich, Hönggerberg Campus, Wolfgang-Pauli-Strasse 10, CH-8093, Zurich, Switzerland.
[6] To whom correspondence should be addressed. (e-mail: hmerkle@pharma.ethz.ch)

ABBREVIATIONS: BSA, bovine serum albumin; CF, 5(6)-carboxyfluorescein; CLSM, confocal laser scanning microscopy; CPPs, cell penetrating peptides; DMEM, Dulbecco's modified Eagle's medium; DOG, 2-deoxyglucose; DPM, disintegrations per minute; ECM, extracellular matrix; FACS, fluorescence-activated cell sorting; FITC, fluorescein isothiocyanate; HBSS, Hank's balanced salt solution; HCT, human calcitonin; HIV-1, human immunodeficiency virus-1; MDCK, Madin Darby Canine Kidney cells; M-β-CD, methyl-β-cyclodextrin; NaN_3, sodium azide; NLS, nuclear localization sequence; PFA, paraformaldehyde; PNA, peptide nucleic acid; SAP, sweet arrow peptide; SV40, simian virus 40; TEER, transepithelial electrical resistance; TJ, tight junctions; ZO-1, zonula occludens protein 1.

considerable interest, and created widespread hopes to exploit the CPP approach for drug delivery purposes, gene therapy and vaccine development (1,2). Various oligocationic cell penetrating peptides, e.g., HIV-1 derived Tat peptides, penetratin (pAntp), oligoarginine peptides or the weakly cationic, human calcitonin derived CPPs and others, have been described in the literature in broad detail (3–7). They were commonly considered for the therapeutic delivery of peptides, proteins, oligonucleotides, plasmids, peptide nucleic acids (PNAs) and even nanoparticles (8–13).

In this study, we investigate the cellular entry of two recently developed, N-terminally carboxyfluorescein (CF) labelled, oligocationic CPPs. One is a branched derivative of the linear human calcitonin derived CF-hCT(9-32) (7), denoted as CF-hCT(9-32)-br, that carries an oligocationic, SV40 derived nuclear localisation sequence, the GPDEVKRKKKP motif, in the form of a side-branch to the main peptide chain (see Table I) (14). The other one is the proline-rich sweet arrow peptide CF-SAP (see Table I), a linear trimer of repetitive VRLPPP domains, and conceived as an amphipathic version of a polyproline sequence related to γ-zein, a storage protein of maize (15–17). The internalization of both CPPs into HeLa cells was recently found to follow the pathway of lipid raft-mediated endocytosis prior to endosomal escape (18).

Diverse mammalian cell lines have been used to study the internalization of CPPs across the plasma membrane. In the majority of cases, "leaky" cell models, such as HeLa, KB 3-1, Bowes Human Melanoma or MC57 fibrosarcoma cells, have been used for CPP internalization (19–23). When cultured on solid surfaces such cell lines lack the ability to form tight junctions and form cell layers of high permeability (24). Cellular models with junctional complexes bear more relevance for therapeutic considerations, namely for the delivery of CPP-cargo constructs into epithelia. Therefore, part of our recent research has been concentrated on internalization studies in epithelial like models with fully developed tight junctions (7). One of the best characterized epithelial models derives from the Madin-Darby canine kidney (MDCK) cell line. When grown to confluence, MDCK cells feature key elements of well-differentiated, polarized epithelia, such as apical–basolateral polarization and tight junctions. Therefore, MDCK monolayers represent an established *in vitro* model for various absorptive and respiratory epithelia (25,26). The architecture of the plasma membrane of polarized epithelial cells is well characterized (27,28). Epithelial cells are connected by a junctional complex encircling the apex of each cell. Tight junctions are the most apical structure of the junctional complex which also includes adherens junctions, desmosomes and gap junctions. Tight junctions constitute a barrier to the paracellular diffusion of solutes from the lumen to the tissue parenchyma (gate function) and restrict the lateral exchange of lipids and proteins between the apical and basolateral plasma membrane domains (fence function) (29–33).

Cell line dependence of CPP internalization has been suggested by different research groups (7,23,24). Previously, Hallbrink *et al*. (34) hypothesized about a cell density dependent internalization of CPPs. In the present study, we demonstrate a differentiation state dependence of the process and efficiency of internalization. With proliferating MDCK we observed marked endocytic internalization of two CPPs by a process that is suggested to involve both lipid rafts and clathrin-coated pits. In contrast, for well-differentiated, confluent MDCK monolayers we noted a massive slow-down of compound unspecific endocytosis and no detectable contribution of lipid raft-mediated endocytosis.

The Rho family of small GTPases, comprising Rho, Rac and Cdc42, are ubiquitously expressed across eukaryotes where they act as molecular switches, cycling between an active GTP-bound state and an inactive GDP-bound state (35,36). In the active state, they interact with various downstream effectors and regulate a variety of cellular events such as actin polymerization, cell morphology and polarity, cell growth control, transcription and membrane trafficking events such as endocytosis (37–42). They are ideally placed to mediate the signalling interface between endocytic traffic and the actin cytoskeleton (43,44). Considering the close apposition between the perijunctional F-actin ring and the epithelial tight junction complex, it is conceivable that Rho-GTPases, through cytoskeletal modification, could affect epithelial barrier function (45). In the present study, we investigated the contents of GTP-bound, active form Rho-A and Rac-1, respectively, in 1 day old MDCK cells with low or high seeding density as well as in 10 day old, well-differentiated MDCK cells with high cell culture density, in order to elucidate a potential relationship between cellular differentiation and endocytic activity, respectively, and Rho-GTPase activation. In fact, we found correspondence between endocytic internalization and active form Rho-A; vice versa, cell density, cellular differentiation and endocytic slow-down were observed to relate with active form Rac-1. To our knowledge, this is the first study that casts light on the role of Rho-GTPases for the differentiation restricted endocytosis of CPPs into an epithelial cell model.

The correspondence between endocytic slow-down and cellular differentiation was further elaborated using an inflammatory, IFN-γ/TNF-α induced model mimicking inflammatory epithelial diseases. Inflammatory epithelial pathologies such as inflammatory bowel diseases, e.g. Crohn's disease and ulcerative colitis (46–50), or inflammatory airway diseases associated with cystic fibrosis (51) or asthma bronchiale (52), typically show increased cytokine production,

Table I. Name, Sequence, and Origin of the Cell-Penetrating Peptides(CPPs) Used[a]

Name	Sequence	Origin
hCT(9-32)-br	LGTYTQDFNKFHTFPQTAIGVGAP-NH_2	human calcitonin,
	|	
	AFGVGPDEVKRKKKP-NH_2	simian virus 40
SAP	VRLPPP-VRLPPP-VRLPPP	modified maize
Tat(FITC)	GRKKRRQRRRGYK(FITC)C-NH_2	HIV-1

[a] hCT(9-32)-br and SAP were CF-labeled at the N-terminus

and significant barrier dysfunction. In particular, we tested whether the internalization efficiency of the investigated CPPs is enhanced when studied in a cytokine pretreated, inflammatory MDCK model, possibly triggered by a cytokine induced redistribution of lipid rafts. Altogether, our findings emphasize the importance of relevant cell models to study CPP internalization and point towards inflamed epithelia as potential niche for CPPs as drug delivery vehicles.

MATERIALS

MDCK cells (low resistance, type II) were kind gifts from the Biopharmacy group (ETH Zurich, Switzerland). Cell culture media, trypsin-EDTA, penicillin, streptomycin and Hank's Balanced Salt Solution (HBSS) were from Gibco (Paisley, UK). Phosphate buffer solution (PBS, pH 7.4) without calcium and magnesium were from Life Technologies (Basel, Switzerland). Foetal calf serum (FCS) was purchased from Winiger AG (Wohlen, Switzerland). Hoechst 33342, cholera toxin subunit B (recombinant), Alexa Fluor 594 conjugate and tetramethylrhodamine-labelled transferrin were from Molecular Probes (Leiden, The Netherlands). 5(6)-carboxyfluorescein (CF), Trypan blue, sodium azide (NaN_3), Triton X-100, 2-deoxy-glucose, Tris(hydroxymethyl)-aminomethane hydrochloride, Tween 20 and bovine serum albumin (BSA) were obtained from Fluka (Buchs, Switzerland), and methyl-β-cyclodextrin (M-β-CD) from Wacker-Chemie (Munich, Germany). EZ-Detect Rho and Rac1 activation kits as well as Halt Protease Inhibitor Cocktail (EDTA free) were from Perbio Science (Lausanne, Switzerland). The polyclonal primary antibody rabbit Anti-ZO-1 was from Zymed Laboratories (South San Francisco, CA), the secondary antibodies goat anti-rabbit Texas red and goat anti-mouse conjugated with horseradish peroxidase were from Jackson ImmunoResearch Laboratories (West Grove, PA). *E. coli* derived recombinant canine interferon-gamma (IFN-γ) and tumor necrosis factor-alpha (TNF-α) were obtained from R&D Systems (Minneapolis, MN). Filter inserts (polyethylene terephthalate (PET), 0.4 μm pore size), companion 12 well plates, 24 well plates and 5 ml polypropylene round-bottom tubes (FACS tubes) were purchased from Falcon (Becton Dickinson Labware, Franklin Lakes, NJ). 96 well plates and glass chamber slides were obtained from Nunc (Roskilde, Denmark). MTT (3-[4,5-dimethylthiazol-2-yl]-2,5-diphenyltetrazolium bromide), Fluorescein isothiocyanate-dextran (FITC-dextran, MW 4400), mouse anti-actin, sodium dodecyl sulphate (SDS) and Bradford reagent were from Sigma (St. Louis, MO). Cell culturing flasks (25 and 75 cm^2) were from TPP (Trasadingen, Switzerland). Centricon centrifugal filter devices were obtained from Millipore (Billerica, MA). ECL Plus Western Blotting Detection Reagent was from Amersham Biosciences (Uppsala, Sweden). [^{3}H]-mannitol (19.7 Ci/mmol) was from Perkin Elmer (Boston, MA). Coverslips and microscope slides were purchased from Knittel (Braunschweig, Germany).

METHODS

Peptide synthesis. Investigated CPPs are listed in Table I. The branched human calcitonin (hCT) derived CPP (hCT(9-32)-br was synthesized by the peptide synthesis unit of the University of Barcelona (Barcelona, Spain). This peptide is derived from the human calcitonin fragment hCT(9-32) and is equipped with the nuclear localization sequence (NLS) of simian virus 40 large T antigen in the side chain of K18 (14). N-terminal fluorescently labelled sweet arrow peptide (CF-SAP) was synthesised by solid-phase peptide synthesis on a 2-chlorotrityl resin following the 9-fluorenyl methoxy carbonyl/*tert*-butyl (Fmoc/*t*Bu) strategy prior to fluorescent labeling with 5(6)-carboxyfluorescein (CF) (16). Finally, a FITC labelled Tat peptide with the sequence GRKKRRQRRRGYK(FITC)C–NH_2 (MW 2237) was synthesized and purified as described previously (53).

Cell culture. MDCK cells were cultured under standard conditions in minimum essential medium with Earl's salts (MEM) containing 10% heat-inactivated FCS and 1% penicillin/streptomycin. Cells were used between passage numbers 227 and 237. For internalization experiments, if not otherwise indicated, cells were seeded at a constant density of 2×10^4 cells/cm^2 on Transwell filters in 12 or 24-well plates or on chamber glasses and incubation was at 37°C. Cells were used in both proliferating and confluent states, starting from 12 h post seeding until 10 days post seeding. For detection of filter grown cells, filters were cut out, put upside down on coverslips and mounted in Dako mounting medium. Cell numbers were determined with a haemocytometer (Assistent, Sondheim/Rhön, Germany). Throughout the study, all experiments were performed in triplicate ($n = 3$), unless otherwise indicated.

Confocal laser scanning microscopy (CLSM) of CPP internalization. MDCK cells were incubated with serum free MDCK medium containing either CF-SAP (50 μM), CF-hCT(9-32)-br (30 μM) or unconjugated fluorophore (50 μM or 30 μM, respectively) for 1 h under horizontal mechanical shaking at 150 min^{-1}. After 30 min, Hoechst 33342 was added to a final concentration of 1 μg/ml for nuclear staining.

To inhibit endocytosis, 1 or 10 day old cells were pretreated for 1 h with NaN_3/2-deoxyglucose (0.1%/50 mM in HBSS) prior to incubation with CPPs. To study the temperature dependence on internalization, studies were carried out at 4 and 37°C. For colocalization studies, cells were co-incubated apically for 30 min in solutions of CF-SAP (50 μM) or CF-hCT(9-32)-br (30 μM) with either cholera toxin (10 μg/ml) or transferrin (50 μg/ml) in serum free MDCK medium.

Subsequently, all samples were washed with phosphate buffered saline (PBS), fixed in 1% (w/v) aqueous paraformaldehyde (PFA) solution for 30 min and washed again. To exclude artifacts owing to cell fixation, preliminary experiments were also performed in unfixed, living cells. Both protocols led to identical vesicular distributions of the two CPPs as well as to identical colocalization patterns with transferrin and cholera toxin. Therefore, we followed a mild fixation protocol with 1% PFA for better handling and to definitively terminate the experiments. Cellular uptake was visualized using a TCS-SP2 laser scanning confocal microscope (Leica Microsystems, Mannheim, Germany) with a 63×, 1.4 NA, plan-apochromatic lens using HeNe 594 nm, HeNe 543 nm, Ar 488 and diode 405 nm lasers. To avoid cross talk, emission signals were collected independently. 3-D multichannel image processing was performed using the IMARIS software (Bitplane AG, Zurich, Switzerland) on a Silicon graphics workstation. Background fluorescence was determined by analysing unlabelled cells. The images were

deconvolved using Huygens software (Scientific Volume Imaging B.V., Hilversum, Netherlands). Colocalization images were obtained by the colocalization program of IMARIS software (Bitplane AG, Zurich, Switzerland).

Internalization and endocytosis inhibition study by FACS. Individual MDCK cultures were used for experiments after 12 h, 1 day and then every 24 h until 10 days post seeding. Cells were incubated from either the apical or the basolateral side with CF-SAP (50 μM), hCT(9-32)-br (30 μM) or unconjugated fluorophore (50 μM or 30 μM, respectively) in serum free MDCK medium for 3 h.

Additional experiments were performed, incubating MDCK cells with 30 μM FITC-dextran, 5 μM Tat peptide, and 30 μM hCT(9-32), respectively, from the apical side or 30 μM transferrin from the basolateral side for 3 h. After incubation, cells were washed, trypsinized for 10 min, resuspended in medium and immediately put on ice. To quench potentially remaining external fluorescence, Trypan blue was added to the samples prior analysis by FACS on a FacScan (Becton Dickinson, Franklin Lakes, NJ) or a FACSCalibur (Becton Dickinson, Franklin Lakes, NJ) within 2 h after trypsinization. A total of 10,000 cells per sample were analyzed. The mean fluorescence intensity of peptide-labelled cell populations was normalized to unlabelled control cells and compared to control cells labelled with 5(6)-carboxyfluorescein.

To study the effects of seeding and cell culture density in MDCK layers, FACS studies were performed comparing half or 1 day old cells with a low seeding density of 2×10^4 cells/cm^2, half or 1 day old cells having a high seeding density of 5×10^5 cells/cm^2, and, finally, 10 day old cells with a low initial seeding density of 2×10^4 cells/cm^2 but a high final cell culture density of 5×10^5 cells/cm^2, after 10 days. Cells were incubated from the apical side with CF-SAP (50 μM), hCT (9-32)-br (30 μM) or unconjugated fluorophore (50 μM or 30 μM, respectively) in serum free MDCK medium for 3 h. Quantification was performed as described above.

For inhibition of endocytosis, 1 or 10 days old cells were pre-treated for 1 h with NaN_3/2-deoxyglucose (0.1%/50 mM in HBSS) or M-β-CD (10 mM in serum free MDCK medium) prior to incubation with CPPs. Statistical significance of internalization was evaluated by pairwise t tests ($n = 3$). Furthermore, temperature-dependent internalization was studied at 4 and 37°C.

ZO-1 staining monitored by CLSM. MDCK cells seeded on filter inserts in 12-well plates were incubated with 1 μg/ml Hoechst 33342 to stain the nuclei. After several washing steps, cells were fixed for 30 min in 1% (v/v) PFA and permeabilized with 0.1% Triton X-100 in PBS for 1 min. Non-specific binding sites were blocked by incubating for 30 min with 1% BSA in PBS. Cells were then incubated for 1 h with polyclonal antibody rabbit anti-ZO-1 (0.5 μg/ml) in 1% BSA in PBS. After another washing step, cells were incubated with goat anti-rabbit Texas red (4 μg/ml) in 1% BSA in PBS for 1 h and washed again. Cells were scanned as described for colocalization studies. As control experiments, cells incubated with secondary antibodies without primary antibody staining confirmed the high specificity of the antibodies.

To investigate the ZO-1 distribution in the inflammatory epithelial model, 10 day old MDCK cells were treated for 24 h with a combination of 100 ng/ml IFN-γ and 1 ng/ml TNF-α in the apical and basolateral compartments, prior to ZO-1 antibody staining as described above and CLSM analysis. For graphical representation of ZO-1 distribution we used the maximum intensity projection as provided by IMARIS software (Bitplane AG, Zurich, Switzerland).

TEER measurement. MDCK cells were cultured as described above. Transepithelial electrical resistance (TEER) was measured in an Endohm tissue resistance measurement chamber (World Precision Instruments, Inc., Sarasota, USA.) and monitored with a Millicell-ERS meter (Millipore/Continental Water Systems, Bedford, USA.) as previously described (54). To obtain values independent of the membrane area, TEER measurements were multiplied by the effective membrane area and reported as Ω cm^2. All measurements were reported as net TEER (total minus the mean TEER of two cell-free inserts). We also performed TEER measurement in an inflammatory epithelial model. 10 day old MDCK cells were treated for 24 h with combinations of 10–1,000 ng/ml IFN-γ and 0.1–1,000 ng/ml TNF-α in the apical and basolateral compartments, prior to TEER measurement as described above. After a cytokine treatment for 2 days, IFN-γ and TNF-α were removed, cells washed with PBS and TEER recovery was measured.

Measurement of active form Rho-A and Rac-1 (pull-down assay and Western blot analysis). Active-form Rho-A or Rac-1, respectively, were measured in 0.5, 1 or 10 day old MDCK cell cultures with cell seeding densities as described for density experiments. MDCK cells grown in 75 cm^2 flasks were lysed in lysis buffer plus protease inhibitor (25 mM Tris × HCl, pH 7.5, 1% NP-40, 150 mM NaCl, 5 mM MgCl2, 1 mM DTT, 5% glycerol, 1 μg/ml each of aprotinin and leupeptin, and 1 mM PMSF) and clarified by centrifugation at 16,000×g at 4°C for 15 min. Cell lysates were incubated with GST-Rhotekin-RBD or GST-human Pak1-PBD to pull down active Rho-A or Rac-1 in the presence of Swell Gel immobilized glutathione at 4°C for 1 h. After incubation, the mixture was centrifuged at 8,000×g to remove unbound proteins. The resins were washed several times with lysis buffer and the sample was eluted by adding 50 μl of SDS sample buffer (5% β-mercaptoethanol, 125 mM Tris × HCl, pH 6.8, 2% glycerol, 4% SDS (w/v) and 0.05% bromophenol blue) and boiling at 95°C for 5 min. 20 μl of the sample volume were analyzed by SDS page and transferred to a nitrocellulose membrane. Unfractionated cell lysates were included for protein quantification and to verify that the Western blot analysis functioned properly. Active Rho-A and Rac-1 were detected by using a specific mouse monoclonal anti-Rho (0.7 μg/mL) or anti-Rac1 (0.5 μg/mL) antibody. Goat anti-mouse antibody conjugated with horseradish peroxidase (0.04 μg/mL) was used as the secondary antibody. To ensure equal protein content of the samples, actin was quantified by a specific mouse monoclonal anti-actin antibody (0.04 μg/mL). Detection was performed with Chemiluminiscent Substrate followed by exposure to X-ray film (average exposure time was 10 s to 5 min). All assays were run in triplicate using independent samples.

Bradford test. To normalize for protein content for all samples of active form Rho-A or Rac-1 analyses, we determined protein contents by performing Bradford tests as described by the manufacturer. Absorption was measured at 570 nm using a ThermoMax microplate reader (Molecular Device, Sunnyvale, CA).

CPP internalization in an inflammatory MDCK model as studied by FACS. Filter grown 10 day old MDCK cells were treated with MDCK medium containing 10–1,000 ng/ml IFN-γ and 0.1–1,000 ng/ml TNF-α for 24 h. Cytokines were present in both the apical and the basolateral media. After washing, cells were incubated from the apical side with CF-SAP (50 μM), hCT(9-32)-br (30 μM), Tat peptide (5 μM) or unconjugated fluorophore (50 μM or 30 μM, respectively) in serum free MDCK medium for 3 h. FACS analysis was performed as described previously. Pairwise *t* tests were performed to reveal the significance of an increase in internalization between untreated and cytokine treated cells (1,000 ng/ml IFN-γ/10 ng/ml TNF-α) ($n = 3$).

Influence of cholesterol depletion in the inflammatory model was studied by pre-treating cells for 1 h with M-β-CD (10 mM in serum free MDCK medium) prior to incubation with CPPs. Pairwise *t* tests were performed to reveal the significance of a decrease in internalization between untreated and M-β-CD treated cells ($n = 5$).

Cytotoxicity assay. An MTT assay was performed to measure cell viability in the described inflammatory model. 10 day old MDCK cells seeded in 96-well plates were treated with cytokine solutions of 10–1,000 ng/ml IFN-γ and 0.1–1,000 ng/ml TNF-α, for 24 h, with 70% EtOH for 7 min or left untreated as control cells. All wells were washed three times with medium and loaded with 100 μl medium. 10 μl MTT reagent (5 mg MTT powder in 1 ml PBS) were added to all wells. After 2 h, the medium was removed and replaced with 100 μl detergent reagent (81% isopropanol, 15% SDS (20%) and 4% 1 M HCl. After additional 4 h, absorbance was measured at 570 nm in a ThermoMax microplate reader (Molecular Device, Sunnyvale, CA).

Transepithelial permeability. 10 day old MDCK cells seeded on filters in 12-well plates were either treated with combinations of 10–1,000 ng/ml IFN-γ and 0.1–1,000 ng/ml TNF-α for 24 h or used as untreated control cells. Prior to permeability measurements, all monolayers were checked for TEER as described above. Confluent MDCK monolayers were equilibrated for 30 min in HBSS, pH 7.4. Monolayers were loaded apically with 0.5 ml HBSS solutions containing 30 μM CF or [^{3}H]-mannitol (4 μCi/ml), respectively and 1.8 ml of HBSS was added to the basolateral side. Blank wells were used as controls. Samples of 100 μl were withdrawn from the basolateral receiver compartment and immediately replaced with the same volume of HBSS at $t = 0$, 1, 2 and 4 h. Effective permeability coefficients of 5(6)-carboxyfluorescein (CF) were determined by direct fluorescence spectrometry (λ_{ex} X492 nm, λ_{em} 517 nm; Varian CARY Eclipse, Zug, Switzerland). CF concentrations transported into the basolateral compartment were extrapolated from a standard curve and expressed as μM cm^{-2} h^{-1} for compound transported. For [^{3}H]-mannitol permeability studies, the samples were mixed with 2 ml scintillation cocktail (Ultima Gold, PerkinElmer Life Sciences, Beltsville, MD) and radioactivity was counted using a liquid scintillation spectrometer from Beckman (Model LS 6500, Fullerton, CA).

RESULTS

CPP internalization in MDCK cells. Cellular internalization of either of the two cationic CPPs (CF-SAP or CF-hCT(9-32)-br) occurred in proliferating MDCK cells 1 day post seeding as shown by CLSM (Fig. 1a or b, left insets, respectively). At this time point the internalized fluorescence featured a punctate pattern indicating localization in discrete vesicular compartments in the cytoplasm typical for endocytosis (55). In contrast, confluent monolayers, 10 days post seeding with well-established cell-to-cell contacts, enabled significantly less internalization (Fig. 1a or b, right insets). The occurence of punctate fluorescence in the cytoplasm was markedly reduced, and the CPPs accumulated mainly in the junctional complex. Unlabelled cells and cells incubated with the fluorescence marker carboxyfluorescein alone were analysed as controls. No cellular fluorescence was observed in both cases (data not shown).

FACS analysis of CPP internalization. To confirm the contrasts in internalization in proliferating versus confluent MDCK cells, we quantified the internalization of CF-SAP

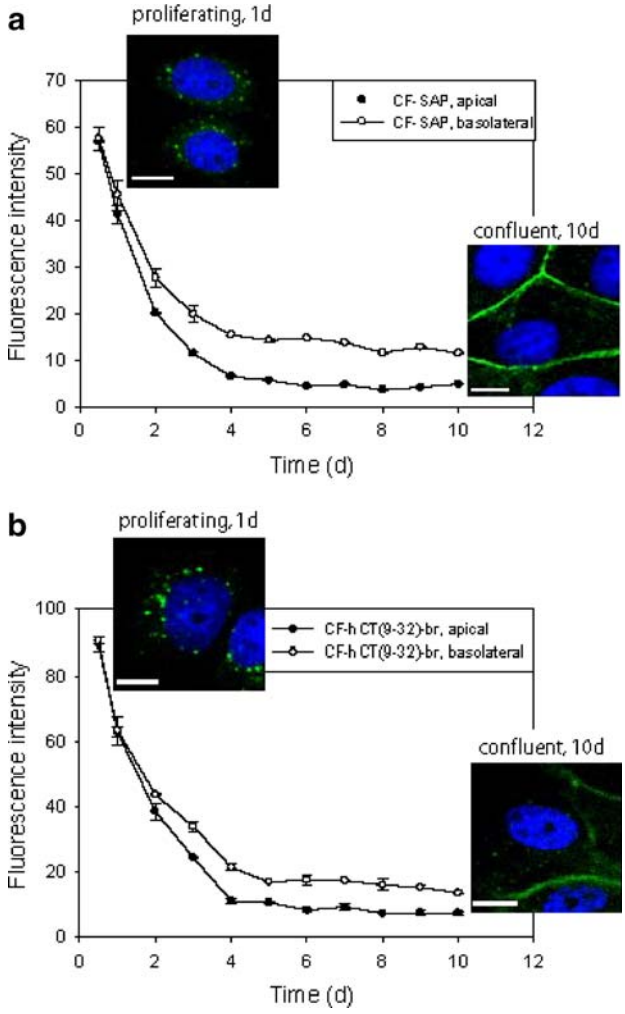

Fig. 1. Internalization of CF-SAP and CF-hCT(9-32)-br in MDCK cells varying in their state of differentiation (FACS and CLSM). MDCK cells from 12 h up to 10 days post seeding were incubated for 3 h with 50 μM CF-SAP (**a**) or 30 μM CF-hCT(9-32)-br (**b**) (FACS). Fluorescence intensities were normalized to control cells of the same age. Inserted CLSM pictures show incubation of 1 or 10 day old MDCK cells with CF-SAP (*1A*, *left or right picture*, respectively) or CF-hCT(9-32)-br (*1B*, *left picture or right picture*, respectively) for 1 h. The scale bar is 10 μm. *CPPs in green*, *nuclei in blue*. Colors indicated in electronic version only.

and CF-hCT(9-32)-br, respectively, by FACS analysis. As shown in Fig. 1a and b, internalization in proliferating MDCK was marked for both CPPs, and similar whether treated from the apical or the basolateral side. With increasing culture time, however, the degree of internalization from both the apical and the basolateral sides decreased strikingly. At confluence, i.e. after a growth period of 4 days, apical internalization reached a baseline level of around one tenth of the initial value and stayed constant for the rest of the growth period. Internalization rates from the basolateral side followed a similar trend but were around twice as high than those from the apical side, probably resulting from the higher surface area of the basolateral membrane. Fluorescence intensities were normalized to untreated control cultures of the same age.

Endocytic internalization into proliferating and confluent MDCK layers. To further identify the internalization mechanisms of CF-SAP and CF-hCT(9-32)-br in proliferating and confluent MDCK cells, we analysed by FACS the internalization under conditions which inhibited endocytosis. Non-treated cells and cells incubated with carboxyfluorescein alone (data not shown) were used as negative controls. At 4°C, internalization of CF-SAP and CF-hCT(9-32)-br, respectively, was strongly reduced in both proliferating and confluent MDCK cells (Fig. 2a and b). Previously, inhibition of endocytosis at 4°C was not only attributed to a blockade of active processes but also to rigidification of lipid membranes at this temperature (56). Therefore, we also tested CPP internalization at 37°C after pre-incubation with NaN_3/2-deoxyglucose, which was expected to impair energy-dependent internalization by ATP depletion. As shown in Fig. 2a and b, internalization of both peptides in proliferating as well as confluent MDCK cells was blocked through pre-treatment with NaN_3/2-deoxyglucose, supporting energy-dependent internalization mechanisms such as endocytosis as the underlying internalization mechanism in proliferating as well as confluent MDCK cells.

Endocytosis in proliferating MDCK cells involves both lipid rafts and clathrin-coated pits. Lipid rafts are defined by their cholesterol enrichment. M-β-CD extracts cholesterol from cell membranes and, therefore, disrupts lipid rafts whereas it does not affect clathrin-dependent endocytosis (57–60). Hence, to investigate involvement of lipid raft dependent internalization of extracellular CF-SAP and CF-hCT(9-32)-br, we pre-treated proliferating MDCK cells with M-β-CD prior to incubation with the CPPs. As shown in Fig. 2a, reduction of intracellular fluorescence was highly significant in proliferating MDCK cells, suggesting lipid raft involvement in the endocytic internalization process. Fluorescence intensities were normalized to untreated control cells.

To confirm this observation, we performed colocalization studies of CF-SAP and CF-hCT(9-32)-br with transferrin and cholera toxin by CLSM. Transferrin is a well-known marker for endocytic internalization via clathrin-coated pits (61,62), whereas cholera toxin exploits clathrin-independent, lipid raft-mediated endocytosis (58–60). To assess whether the two CPPs were internalized via one of these endocytic pathways, CF-SAP and CF-hCT(9-32)-br were each mixed with TRITC-labelled transferrin or Alexa Fluor 594-labelled cholera toxin, respectively, and the binary mixture incubated with proliferating MDCK cells (Fig. 2c). Related colocalization micrographs demonstrate colocalized vesicles of CPPs and transferrin or cholera toxin, respectively (Fig. 2c a′, b′, c′, d′). In detail, Fig. 2c a and a′ shows a corresponding set of experiments with CF-SAP and cholera toxin, Fig. 2c *b* and b′ with CF-SAP and transferrin, Fig. 2c *c* and c′ with CF-hCT(9-32)-br and cholera toxin, and finally Fig. 2c *d* and d′ with CF-hCT(9-32)-br and transferrin. CF-SAP and CF-hCT(9-32)-br showed partial colocalization with both cholera toxin and transferrin, suggesting an involvement of lipid rafts as well as clathrin-dependent endocytosis in the internalization of CF-SAP and CF-hCT(9-32)-br into proliferating MDCK cells. In fact, we calculated colocalization rates of the two peptides with either one of the two endocytosis markers of about 35–54% (data not shown). Taken together, our results indicate in a consistent fashion that CF-SAP and CF-hCT(9-32)-br are internalized by proliferating MDCK cells via endocytosis. Both lipid rafts and clathrin-coated pits are suggested to be involved. For the rest of this work we focus exclusively on the lipid raft mediated pathway.

Endocytic pathway in confluent MDCK cells. To further investigate the involvement of lipid rafts in the endocytosis of CF-SAP and CF-hCT(9-32)-br by confluent MDCK, we pre-treated cell layers with M-β-CD prior to incubation with the peptides. Fluorescence intensities were normalized to untreated control cells. As shown in Fig. 2b, reduction in intracellular fluorescence was only marginal in the case of CF-hCT(9-32)-br and absent for CF-SAP (Fig. 2b). As there was only low internalization of CF-SAP and CF-hCT(9-32)-br into confluent MDCK cells, colocalization experiments with endocytosis markers did not yield unequivocal results, neither in favour nor against involvement of lipid rafts (data not shown).

Compound unspecific endocytic slow-down. We next addressed the question whether the observed endocytic slow-down in CPP internalization was a distinct phenomenon for CF-SAP and CF-hCT(9-32)-br, or an unspecific feature of endocytosis in confluent MDCK cells. FITC-dextran and TRITC-labelled transferrin are well known markers of endocytosis, whereas CF-hCT(9-32) and FITC-labelled Tat have been previously reported to be taken up by endocytosis (7, 62–64). Filter grown MDCK cell cultures ranging from 12 h to 10 days post seeding were incubated with solutions of FITC-dextran, TRITC-labelled transferrin, CF-hCT(9-32) and FITC-labelled Tat, respectively. Fluorescence intensities were normalized to untreated control cells of the same age. Fig. 3 shows all compounds to be readily taken up in proliferating MDCK cells whereas the degree of internalization decreased markedly with increasing culture time. These findings suggest that the observed slow-down in the endocytosis of the two investigated CPPs in confluent MDCK cells is compound unspecific.

Relation of endocytic slow-down with increasing cell density and formation of tight junctions. Effects of seeding and cell culture density. To evaluate whether seeding and cell culture densities had an impact on CPP internalization efficiency in MDCK cells, we compared internalization rates of CF-SAP and CF-hCT(9-32)-br, respectively, in half or one day old MDCK cells of low or high seeding density, as well as in 10 day old, well-differentiated cell cultures with low seeding density but high final cell culture density. As shown in Table II, internalization into cell layers with high initial

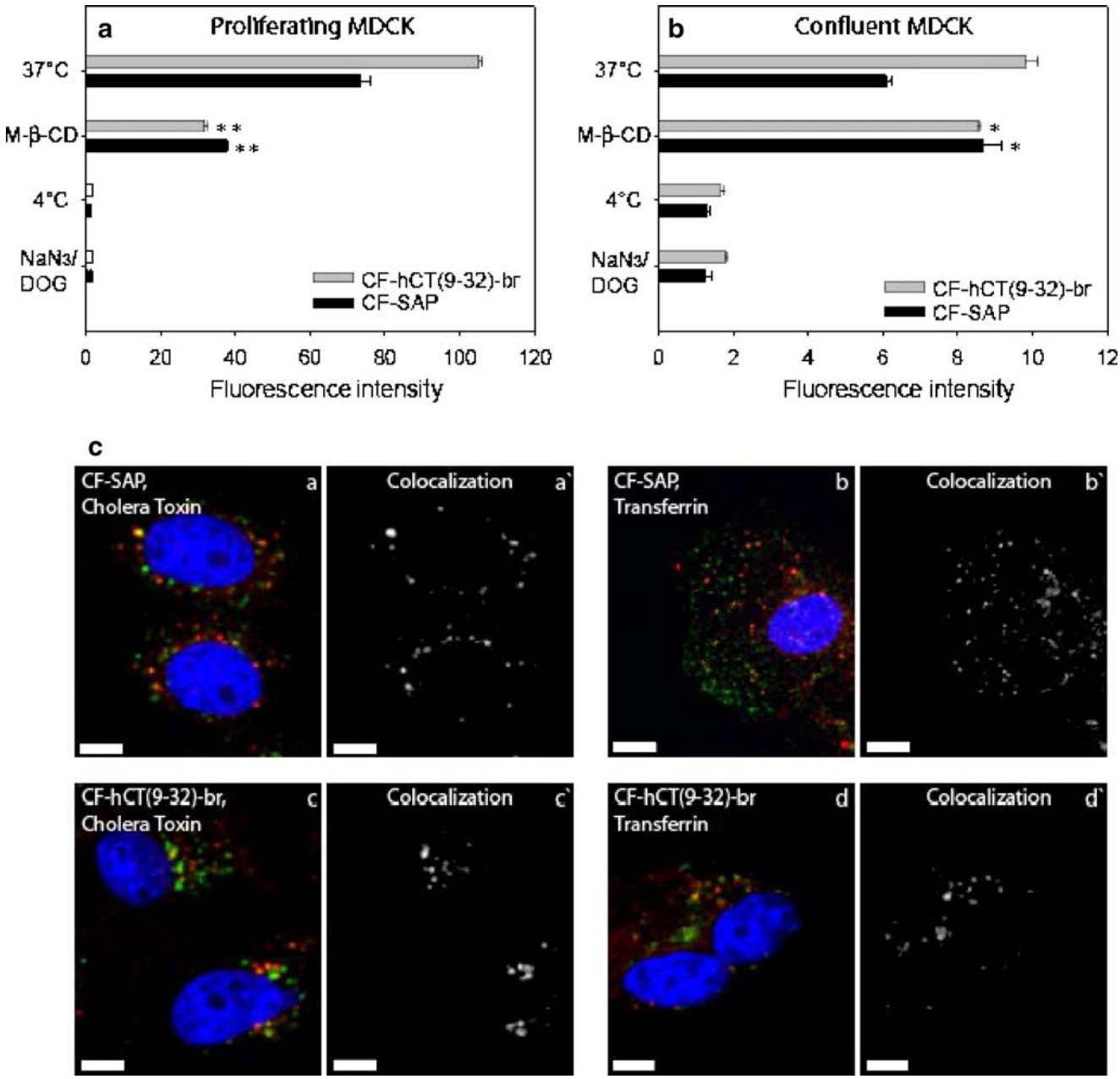

Fig. 2. Internalization and endocytosis inhibition of CF-SAP or CF-hCT(9-32)-br in MDCK cells (FACS). Proliferating MDCK cells (**a**) and confluent MDCK cell (**b**) were incubated for 3 h at either 37 or 4°C with 50 μM CF-SAP (*black bars*) or 30 μM CF-hCT(9-32)-br (*grey bars*). Endocytosis inhibition was performed by pre-treating cells with 10 mM M-β-CD or 0.1% NaN_3/50 mM 2-deoxyglucose (NaN_3/DOG) prior to incubation with CF-SAP or CF-hCT(9-32)-br. Fluorescence intensities are normalized to control cells. Significant and highly significant results for the reduction of internalization through M-β-CD are indicated as * or ** (*t* test, $n = 3$). Colocalization study of CF-SAP and CF-hCT (9-32)-br with cholera toxin or transferrin, respectively in proliferating MDCK cells. (**c)** Colocalized vesicles in *yellow*, peptides (CF-SAP or CF-hCT(9-32)-br) in *green* and endocytosis markers (cholera toxin and transferrin) in *red*. Cells were incubated with 50 μM CF-SAP or 30 μM CF-hCT(9-32)-br and simultaneously stained with 10 μg/ml cholera toxin or 50 μM transferrin, repectively, for 30 min. Colocalization of both CF-SAP and CF-hCT(9-32)-br with cholera toxin suggests lipid raft-mediated endocytosis (**a**,**c**). Colocalization with transferrin suggests clathrin-mediated endocytosis (**b**,**d**) for both peptides. **a** CF-SAP and cholera toxin. **b** CF-SAP and transferrin. **c** CF-hCT(9-32)-br and cholera toxin. **a′**, **b′**, **c′** and **d′** (CF-hCT(9-32)-br and transferrin) represent related overlay micrographs showing colocalized vesicles in white. The scale bar is 7 μm. Colors indicated in electronic version only.

seeding density was much lower than in those of low seeding density of the same age (~84% less internalization) indicating a marked impact of cell seeding density on internalization efficiency. Still, half or one day old cells with high seeding density feature slightly higher internalization rates than 10 day old MDCK cells with a low seeding density but a high final cell culture density (~92% less internalization). Fluorescence intensity of 0.5 day old, low density cells was set to 100%.

TEER measurements. To demonstrate a functional coincidence between the endocytic slow-down of CPP internalization and the development of the tight junctional network in the MDCK cultures we monitored their TEER values during

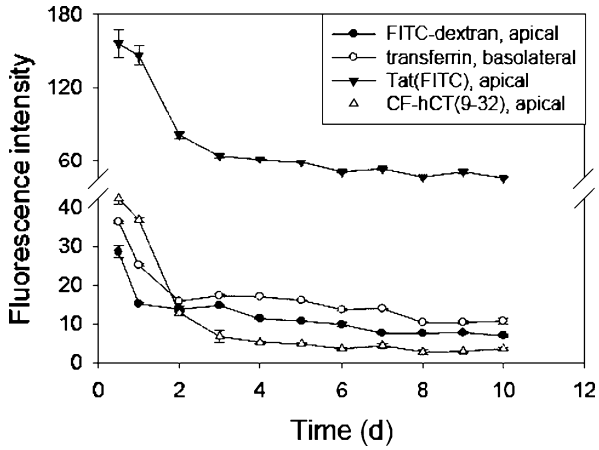

Fig. 3. Endocytic internalization into MDCK cells varying in differentiation states (FACS). MDCK cells ranging from 12 h to 10 days post seeding were incubated for 3 h with 30 μM FITC-dextran, 5 μM Tat(FITC) or 30 μM CF-hCT(9-32)-br from the apical side and with 30 μM transferrin from the basolateral side. Fluorescence intensities were normalized to untreated control cells of the same age.

the growing period of 10 days. As shown in Fig. 4a, TEERs increased initially and then dropped to a stable value of around 130 Ω cm^2 after 4 or 5 days.

Tight junctional protein ZO-1 staining. For the same purpose as with the TEER measurements, we performed ZO-1 staining in MDCK cell cultures from day 1 until day 10 post seeding. As shown in Fig. 4b, soon after seeding cells begin to form small cell clusters and establish first cell-to-cell contacts. Formation of tight junctions immediately started where cells came into contact, particularly at the corners between the cells. Day after day, with increasing cell cluster size, more cell-to-cell contacts were established and after day 4 post seeding a coherent tight junctional network was formed. At that time point, CPP internalization had yet reached a lower level and stayed constant for the rest of the growth period (see Fig. 1a and b). Until day 10 post seeding, cell culture density continued to increase, resulting in a fully organized and polarized tightly packed monolayer. Taken together, the observed endocytic slow-down relates directly with cell density and the formation of a coherent tight junctional network.

Monitoring active form Rho-A and Rac-1. Rho-family GTPases have been previously demonstrated to be intimately involved in the regulation of endocytic traffic and cellular differentiation (36,65). To elucidate a potential relationship between cellular differentiation and endocytic activity, respectively, and Rho-GTPase activation in MDCK cells, we investigated the expression levels of GTP-bound, active form Rho-A and Rac-1, respectively, in one day old MDCK cells with low or high seeding density as well as in 10 day old, well-differentiated MDCK cells with high cell culture density. As shown in Fig. 5a and c, the contents of total Rho-A and Rac-1, respectively, in all three samples were alike, confirming the equal protein content of all samples measured by a Bradford test. One day old, low density cells showed the highest contents of active form Rho-A, whereas active Rho-A was strongly reduced in 1 day old, but high density cells, and almost abolished in 10 day old MDCK cells (Fig. 5a). For Rac-1, inverse activities were observed: almost no active Rac-1 was found in 1 day old, low density cells, slightly higher contents in 1 day old, high density cells, and high contents in 10 day old MDCK cells (Fig. 5c). Fig. 5b and d show densitometric quantifications of active form Rho-A and Rac-1 when normalized to control values of total Rho-A or Rac-1, respectively. Our data indicate a relationship between endocytic activity and active form Rho-A, as well as between cell density, cellular differentiation and endocytic slow-down, respectively, and active form Rac-1. These findings suggest an involvement of Rho-A and Rac-1 in regulating the endocytosis of the two CPPs in the context of cellular differentiation.

Table II. Fluorescence Intensities (%) of CF-SAP and CF-hCT(9-32)-br in MDCK Cells Varying in Growing Period and Seeding Density

Growing period (Seeding density)	Flourescence intensity (%)	
	CF-SAP	CF-hCT(9-32)-br
0.5 days (2×10^4 cells/cm^2)	100 ± 9.16	100 ± 2.49
1 day (2×10^4 cells/cm^2)	65.61 ± 3.12	64.91 ± 4.47
10 days (2×10^4 cells/cm^2)	7.42 ± 0.14	7.56 ± 0.43
0.5 days (5×10^5 cells/cm^2)	14.94 ± 0.21	18.01 ± 0.78
1 day (5×10^5 cells/cm^2)	8.1 ±0.08	8.72 ± 0.08

Fluorescence intensities are normalized to control cells of the same age.

CPP internalization in an inflammatory MDCK model. To further elaborate our findings towards a relation between endocytic slow-down and cellular differentiation, we studied CPP internalization in MDCK monolayers featuring a compromised tight junctional organization. Therefore, prior to incubation with CPPs, fully organized MDCK monolayers were treated with MDCK medium containing IFN-γ and TNF-α at stepwise increased concentrations. As shown in Fig. 6, CPP internalization was significantly enhanced upon such inflammatory pre-treatment. A combination of IFN-γ and TNF-α provided synergistic effects on epithelial barrier function (66,67), whereas IFN-γ or TNF-α alone were less effective.

Transepithelial permeability and cytotoxicity in an inflammatory MDCK model. To further evaluate the effects resulting from inflammatory cytokine pre-treatments, we determined the transepithelial permeability of CF and [^{3}H]-mannitol in confluent MDCK monolayers with and without prior cytokine pre-treatment. Cell culture inserts featured TEER values of 120 ± 12 Ω cm^2 for untreated MDCK layers. When MDCK monolayers were treated with a IFN-γ/TNF-α mix of 1:100 ng/ml within 24 h, TEER values decreased significantly (36 ± 9 Ω cm^2) and stayed at low values within the investigated time interval of 48 h. Removal of the cytokine mix led to a complete recovery to normal TEER values within 72 h (data not shown).

As demonstrated in Fig. 7a, pre-treatments with IFN-γ/TNF-α increased the permeability of [^{3}H]-mannitol in a time and concentration dependent fashion. This was confirmed by a concomitant increase in CF flux in the same time and concentration dependent manner (Fig. 7b). Cytokine concentrations and application periods correlated directly with disintegrations per minute (DPM) and permeability coefficients, respectively.

To investigate cell viability after cytokine pre-treatment, we performed a series of MTT toxicity assays. Even at the

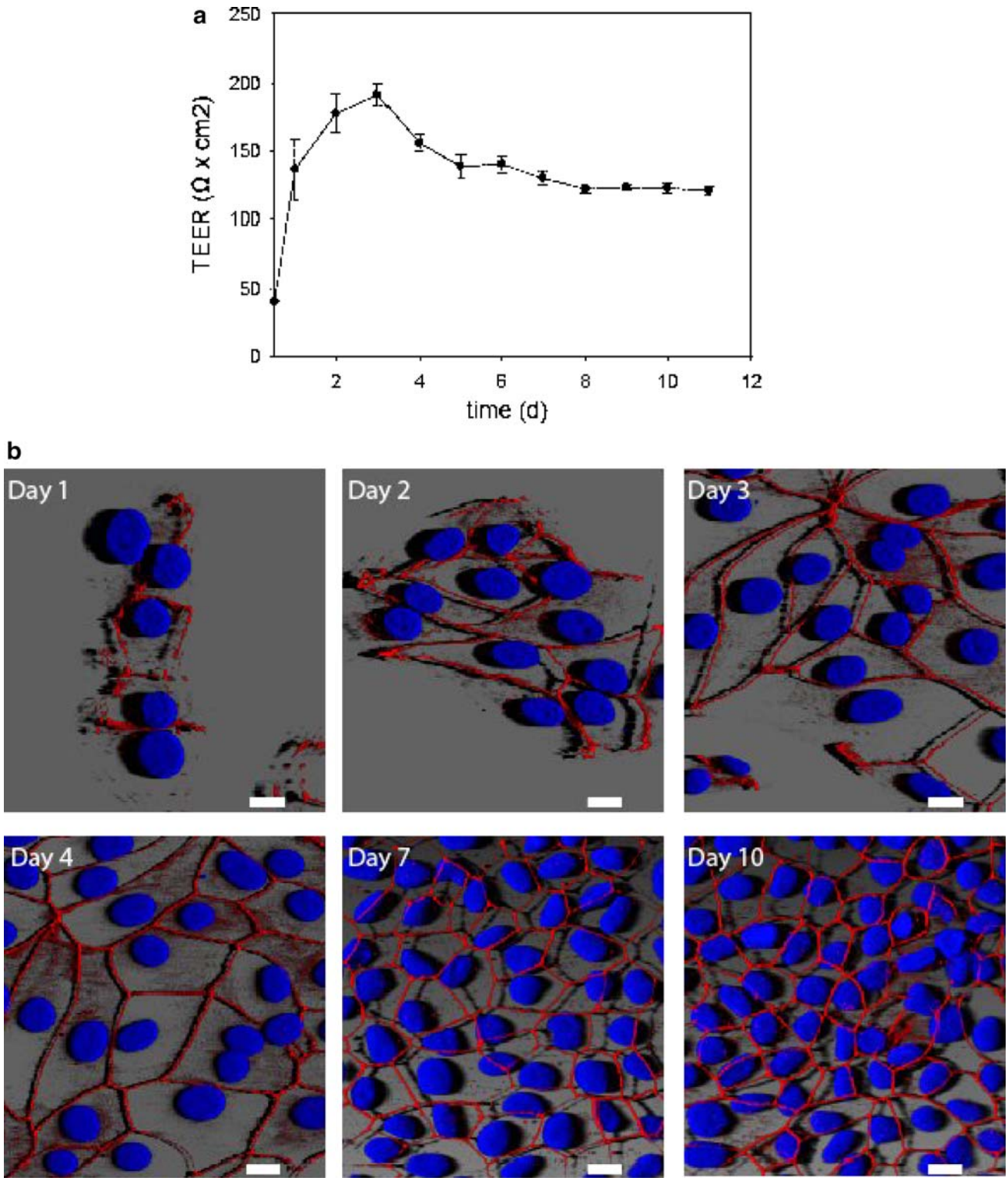

Fig. 4. TEER measurement. (**a**) Transepithelial electrical resistance (TEER) was measured in MDCK cells ranging from 12 h to 10 days post seeding. To obtain values independent of the membrane area, TEER measurements were multiplied by the effective membrane area and reported as $\Omega \times cm^2$. All measurements are reported as net TEER (total minus the mean TEER of two cell-free inserts). Tight junctional plaque protein ZO-1 staining. (**b**) ZO-1 staining was performed in MDCK cells ranging from 12 h to 10 days post seeding. The scale bar is 20 μm.

highest cytokine concentration, i.e. 1,000 ng/ml for each IFN-γ and TNF-α, cell viability was reasonably preserved at 80% as compared to untreated control cells and EtOH treated cells. Viabilities were even better at lower concentrations.

Cytokines induce redistribution of the tight junction protein ZO-1. Cytokine-induced redistribution of tight junction proteins to the membrane has been observed by Bruewer *et al.* (67). To visualize changes in the distribution

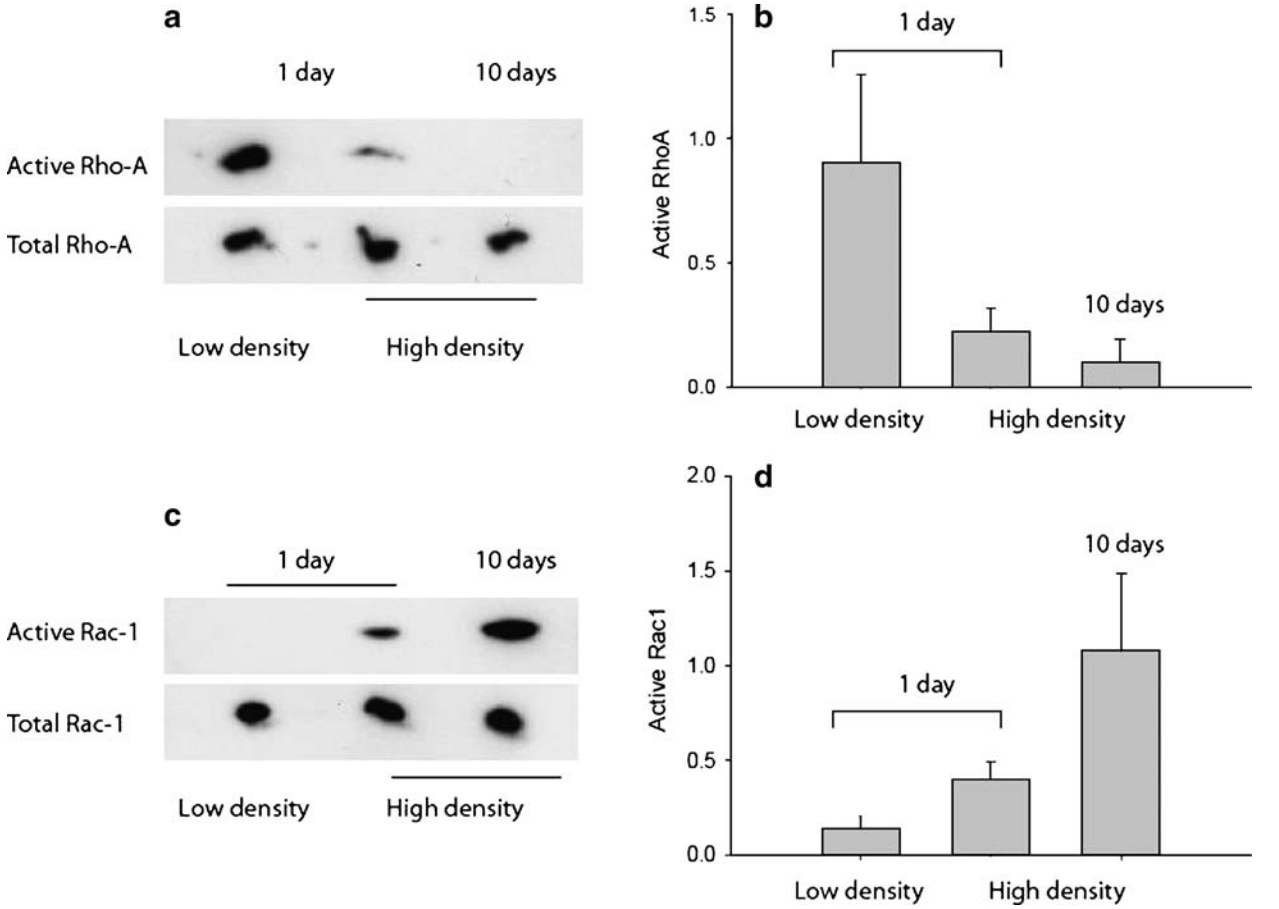

Fig. 5. Active form Rho-GTPases. Contents of GTP-bound, active form Rho-A (**a**) and Rac-1 (**c**), respectively, were measured in 1 day old cells with low or high seeding density as well as in 10 day old, well-differentiated MDCK cells with low seeding density but high final cell culture density and compared to total Rho-GTPase contents. (**b**) and (**d**) show quantification of active form Rho-A and Rac-1 when normalized to control values of total Rho-A or Rac-1, respectively.

of the tight junction protein ZO-1 due to cytokine treatment, we performed ZO-1 staining in cytokine pre-treated MDCK cells (IFN-γ/TNF-α 1:100 ng/ml) and compared it to ZO-1 staining in control cells. As shown in Fig. 8b, cytokine exposure induced redistribution of the plaque protein ZO-1 as compared to control cells (Fig. 8a). Redistribution was in a cytokine concentration-dependent way (data not shown).

Involvement of lipid rafts in enhanced internalization in inflammatory MDCK model. As demonstrated in Fig. 2a and b, lipid rafts play a significant role in the endocytosis of CPPs in proliferating but not in confluent MDCK cells. Cytokine pre-treatments of confluent MDCK restored much of the propensity for lipid raft mediated endocytosis. This is demonstrated by the inhibitory effect of M-β-CD on the internalization of CF-SAP and CF-hCT(9-32)-br in cytokine pre-treated, confluent MDCK. The reduction in CPP internalization was in a cytokine concentration-dependent fashion (Fig. 8c and d). For the studied inflammatory model, a redistribution of tight junction proteins which have been described to be associated with lipid raft microdomains (67,68) might lead to a concomitant restoration of lipid rafts on confluent MDCK cultures, reconstituting the propensity for lipid raft-mediated endocytosis of CPPs.

DISCUSSION

In recent years, increasing numbers of CPPs have been discovered and evaluated for their ability to deliver therapeutics into cells that otherwise cannot translocate cellular membranes. In this work, we investigated the effect of cell density and differentiation state on the internalization kinetics and pathways of two CPPs in epithelial cell models and the thereby observed differentiation restricted endocytic slowdown. In particular, we suggest involvement of Rho GTPases in the endocytosis of CPPs. Furthermore, based on internalization studies in a cytokine induced inflammatory epithelial model, we allude to inflammatory epithelia as potential niche for a clinical future of CPPs as vectors for anti-inflammatory therapeutics.

Up to date, most *in vitro* internalization studies with CPPs were carried out in proliferating, "leaky" cell models devoid of tissular characteristics or junctional complexes (19–23). For our studies we chose the kidney epithelial MDCK cell line. When grown to confluence, MDCK cells feature typical characteristics of polarized epithelia and mimic the epithelial organization of drug absorption sites, such as the respiratory and intestinal mucosae. Quite

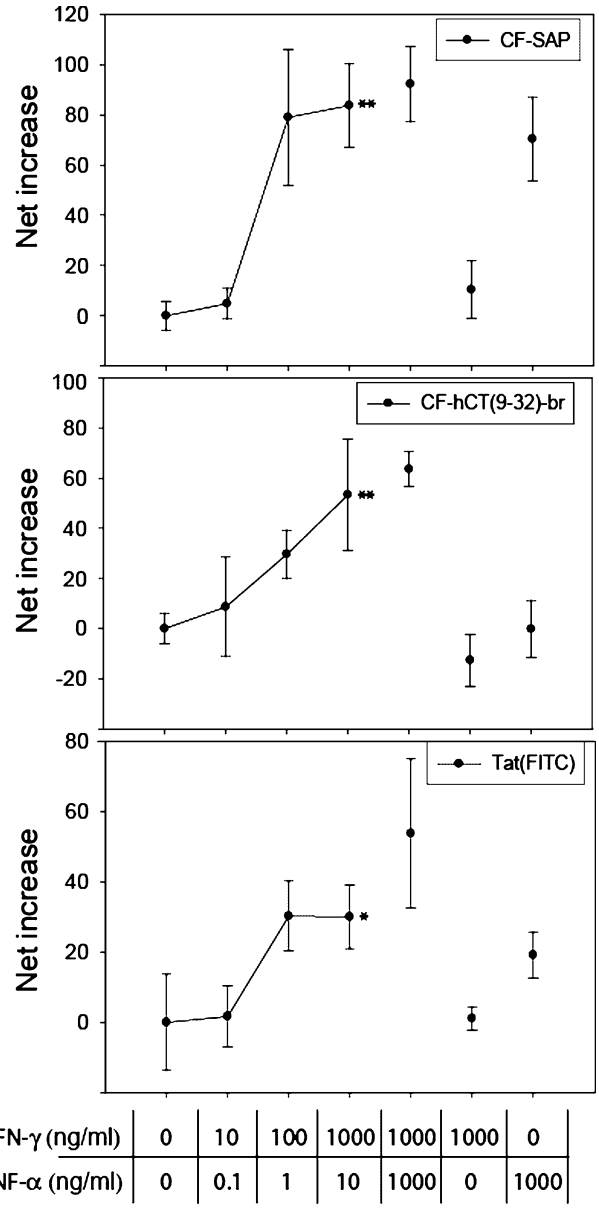

Fig. 6. Net increase of CPP internalization into an inflammatory MDCK model by FACS. Fully organized MDCK monolayers were treated with MDCK medium containing IFN-γ and TNF-α in concentrations ranging from 0–1000 ng/ml, prior to incubation with 50 μM CF-SAP, 30 μM CF-hCT(9-32)-br or 5 μM Tat(FITC) for 3 h. Fluorescence intensities are normalized to control cells. Significant ($p = 0.05$) and highly significant ($p = 0.01$) results are indicated as * or ** (*t* test, $n = 3$).

different to the efficient internalization of Tat peptides into proliferating cell cultures, Violini *et al.* (23) observed a lack of intracellular accumulation of fluorescein conjugated Tat-peptide in confluent MDCK and CaCo-2 cells. By contrast, "leaky" cell models, such as HeLa and KB 3-1 cells, showed cytoplasmic and nuclear accumulation. In one of our previous studies to this subject, using linear human calcitonin derived CPPs, Tat(47-57) and penetratin(43-58), internalization into proliferating HeLa cells was superior to that in a fully polarized and differentiated MDCK model (7). Similarly, Zhang *et al.* (24) suggested a cell type-specific barrier to control the internalization of RI-Tat-9 into HeLa, MT2, MDCK and Caco-2 cells.

Previously we observed marked internalization efficiency in HeLa cells for the linear proline-rich sweet arrow peptide CF-SAP (Table I) (15–17) and the branched derivative of the linear human calcitonin derived CPP CF-hCT(9-32) (7), denoted as CF-hCT(9-32)-br (Table I) (14). Both CPPs were readily taken up by HeLa cells through lipid raft-mediated endocytosis followed by endosomal escape (18). In the current study in proliferating MDCK cells, the data suggested concomitant lipid raft-mediated endocytosis and endocytosis via clathrin coated pits, indicating a cell line specific contrast to the pathway found in HeLa cells. After reaching confluence, however, internalization of the investigated CPPs in MDCK monolayers dropped drastically. Hallbrink *et al.* (34) found similar differences in intracellular MAP and penetratin uptake in CHO cells to correlate to the peptide-to-cell ratio, but due to differences in cell seeding densities, rather than culture time.

Therefore, we investigated in more detail the impact of cellular differentiation on efficiency and mechanism of CPP internalization through lipid raft-mediated endocytosis. By comparing proliferating versus confluent MDCK cell cultures, we found the slow-down in endocytic activity to be related with the increasing cell culture density on the one hand, and the formation of tight junctions on the other. The observed slow-down was not specific for the two investigated CPPs but compound unspecific as it was shared with several common markers of endocytosis.

To find out more about the underlying process controlling the endocytic slow-down of the CPPs, we analysed the occurence of active Rho-GTPases, Rho-A and Rac-1, in MDCK layers of different states of differentiation. Rho-GTPases are known to regulate a variety of cellular events such as actin polymerization, cell morphology and polarity, cell growth control, transcription and membrane trafficking events such as endocytosis (36–42). Apparently, Rho-GTPases mediate the signalling interface between endocytic traffic and actin cytoskeleton and, through cytoskeletal modification, affect epithelial barrier function (43–45). For several cellular functions inverse activities of Rho-A versus Rac-1 and Cdc42 GTPases have been observed (36,62,69,70), such as in actin reorganization and capacity to affect endocytosis. In polarized MDCK cells, Rho-A activation has been found to stimulate apical and basolateral endocytosis whereas Rac-1 activation led to decreases in apical and basolateral endocytosis (69,70). During the formation of epithelia, Cdc42 and Rac-1 play a prominent role in the generation of intimate cell-to-cell contacts (36,71,72). Up until now, the role of Rho GTPases in the endocytosis of CPPs is unknown.

Our findings suggest an involvement of Rho-family GTPases in the differentiation restricted regulation of CPP endocytosis. The extent of CPP uptake was directly related with active form Rho-A, whereas active form Rac-1 related with cell density, cellular differentiation and endocytic slow-down. This reflects the mentioned inverse roles of Rho-A and Rac-1. To our knowledge, this is the first study to cast light on the cell line and differentiation restricted endocytosis of CPPs into epithelial cell models and its underlying cellular mechanism.

We further studied an interesting correspondence between endocytic slow-down and cellular differentiation in an inflammatory MDCK model that was used to mimic inflam-

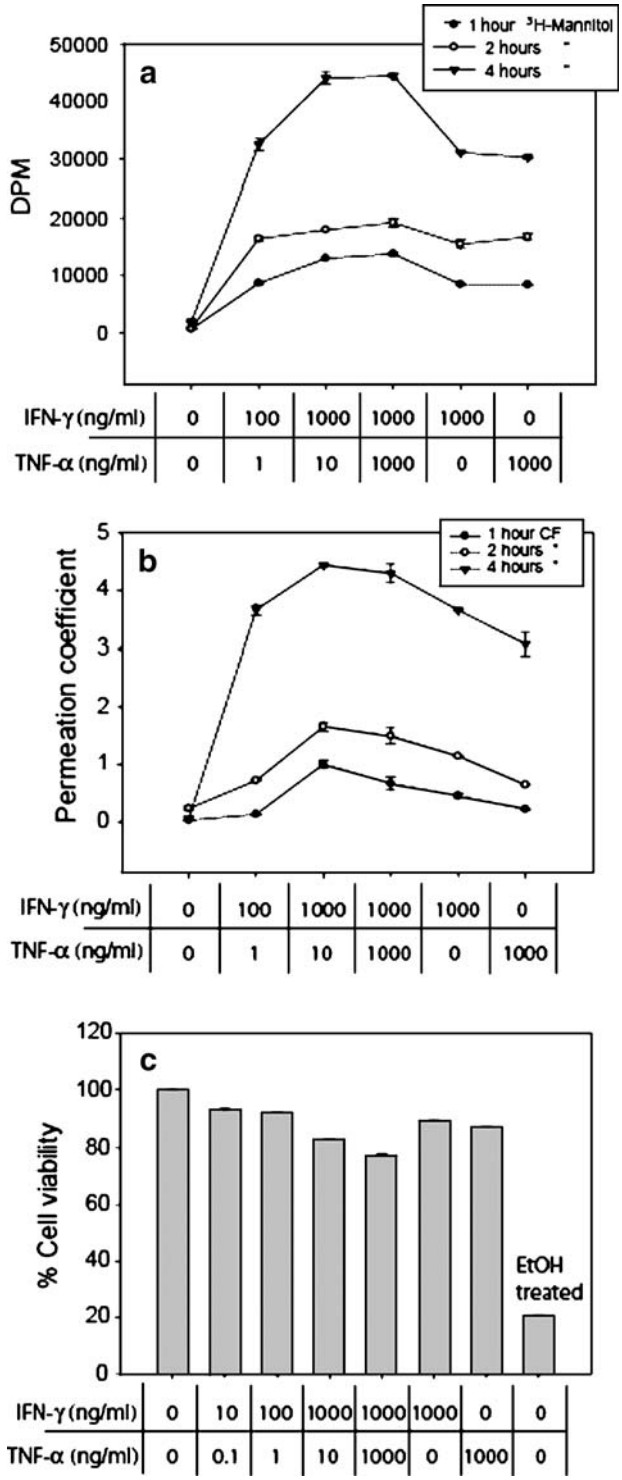

Fig. 7. Transepithelial permeability and cytotoxicity in an inflammatory MDCK model. Transepithelial permeability of [^{3}H]-mannitol (**a**) and CF (**b**) was measured in confluent MDCK monolayers with or without prior pre-treatment with cytokines (IFN-γ and TNF-α in concentrations ranging from 0–1,000 ng/ml). CF concentrations transported into the basolateral compartment were expressed as μM cm^{-2} h^{-1}. (**c**) shows an MTT assay in confluent MDCK monolayers pre-treated with IFN-γ and TNF-α in concentrations ranging from 0–1,000 ng/ml. Untreated control cells and cells treated with EtOH as a positive control were included.

matory pathologies of epithelia. Typically, inflammatory epithelial diseases, such as inflammatory bowel disease, or airway diseases originating from cystic fibrosis or asthma bronchiale, are associated with elevated cytokine production and significant barrier dysfunction (46–52). We found the internalization efficiency of CPPs in the inflammatory MDCK model to be largely enhanced as compared to untreated control. Depending on cytokine concentration, endocytosis of CPP increased by up to almost 90%, concomitant with an increase in permeability of [^{3}H]-mannitol as a marker for paracellular permeability. By analysis of cell viability we could show that enhanced endocytosis and paracellular permeability, secondary to cytokine treatments, were not related to cell death, at least not under the conditions tested. Nevertheless, small transient conductive leaks are likely to occur (73). Fish *et al.* (66) suggested that TNF-α may have synergistic effects on IFN-γ mediated alterations of epithelial cell function. In fact, the combined cytokine treatment of IFN-γ and TNF-α allowed lower concentrations of the cytokines in favour of lower toxicity profiles as compared to non-combined cytokine treatments.

Bruewer *et al.* (67) found the exposure of epithelia to cytokines to induce a redistribution of tight junctional proteins that was not associated with a significant change in the total levels of these proteins, suggesting protein redistribution rather than membrane degradation. Changes in tight junctional functionality have been implicated in the pathogenesis of several inflammatory epithelial diseases. For instance, redistribution of tight junction proteins was observed in patients suffering from active inflammatory bowel disease (IBD), where inflammatory cytokines such as IFN-γ and TNF-α were elevated (74,75). Increased levels of inflammatory cytokines were also found on the bronchial epithelia of cystic fibrosis patients (76) and on the gastric epithelium of patients infected with *Helicobacter pylori* (77). On the cellular level, changes in the integrity of tight junctions in combination with a redistribution of tight junctional proteins were observed in primary human airway epithelial cells from cystic fibrosis patients (51). In line with these findings, we demonstrated that the cytokine pre-treatment of MDCK monolayers led to a redistribution of the tight junctional plaque protein ZO-1 in a concentration dependent way. Previously, Nusrat *et al.* (68) denoted tight junctions as lipid raft membrane microdomains, enriched in cholesterol, and featuring an affiliation of the tight junction proteins with Triton X-100-insoluble membrane rafts. The degree of affiliation was only marginally affected by the cytokine pre-treatment. Furthermore, cytokines did not alter the overall biophysical properties of membrane rafts (67).

The present study suggests lipid rafts to be crucial for the endocytosis of CPPs in proliferating MDCK cells. Contrastingly, they were not measurably involved in the internalization process into confluent layers. Interestingly, when confluent MDCK cells were treated with cytokines, lipid rafts regained their role in mediating the endocytosis of CPPs. In fact, the cellular internalization of both CPPs was markedly reduced—in a cytokine concentration dependent manner—upon extraction of cholesterol with M-β-CD. We thus conclude that—under inflammatory conditions—the redistribution of tight junction proteins associated with lipid

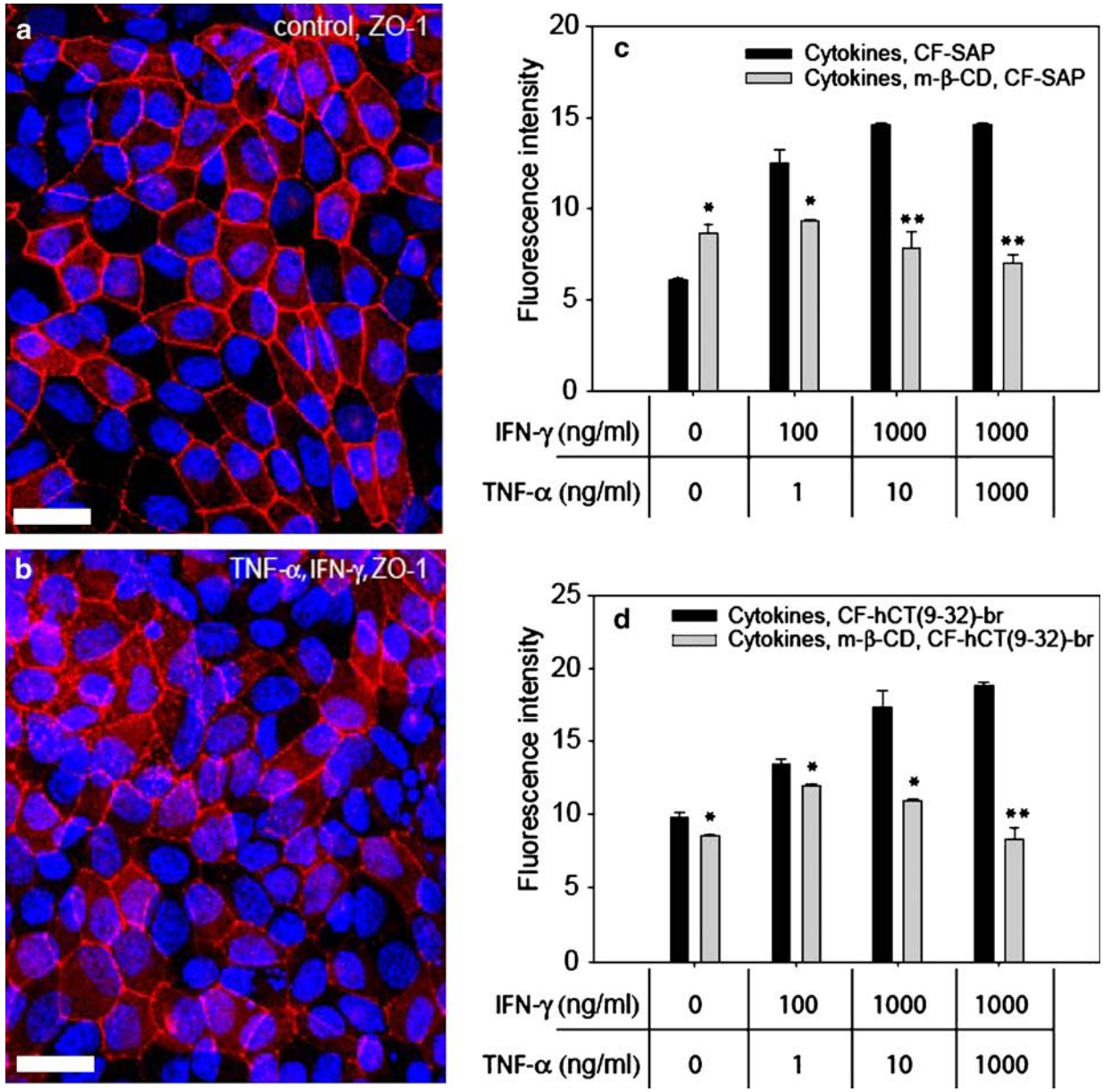

Fig. 8. Distribution of tight junctional plaque protein ZO-1 with or without prior cytokine treatment (CLSM). (**a**) and (**b**) ZO-1 staining in cytokine pre-treated confluent MDCK cells (IFN-γ/TNF-α 100/1 ng/ml) was compared to ZO-1 staining in control cells. Maximum intensity projection is shown. The scale bar is 20 μm. (**c**) and (**d**) MDCK cells were pre-treated with IFN-γ and TNF-α in concentrations ranging from 0–1,000 ng/ml prior to incubation for 3 h with 50 μM CF-SAP (**c**) or 30 μM CF-hCT(9-32)-br (**d**). Additionally, cholesterol depletion was performed by pre-treating cells with 10 mM M-β-CD before incubation with CF-SAP or CF-hCT(9-32)-br. Fluorescence intensities are normalized to control cells. Significant and highly significant results for the reduction of internalization through M-β-CD are indicated as * or ** (*t* test, $n = 5$).

raft microdomains (67,68) re-opens the lipid raft mediated pathway for CPPs in confluent MDCK cells. This observation could make our findings particularly interesting for CPP mediated, targeted delivery of anti-inflammatory drugs and may explain previous empirical observations on the CPP mediated delivery of cyclosporine A to inflammatory epithelia (78) or of caveolin-1 scaffolding domain against vasodilatation and nitric oxide production (79). Nevertheless, the therapeutic potential of this approach has yet to be demonstrated.

ACKNOWLEDGMENTS

The authors acknowledge the following contributions: Professor Randall Mrsny (Welsh School of Pharmacy, Cardiff UK) for valuable discussions on cytokine induced inflammatory cell models. Professor Heidi Wunderli-Allenspach and Dr. Gabor Csúcs (ETH Zurich) for the opportunity to use their confocal laser scanning microscopes, and Ms. Hanna Barman for help and advice with the Western Blot experiments.

REFERENCES

1. M. C. Morris, L. Chaloin, F. Heitz, and G. Divita. Translocating peptides and proteins and their use for gene delivery. *Curr. Opin. Biotechnol.* **11**:461–466 (2000).
2. J. S. Wadia and S. F. Dowdy. Modulation of cellular function by TAT mediated transduction of full length proteins. *Curr. Protein Pept. Sci.* **4**:97–104 (2003).
3. D. Derossi, A. H. Joliot, G. Chassaing, and A. Prochiantz. The third helix of the Antennapedia homeodomain translocates through biological membranes. *J. Biol. Chem.* **269**:10444–10450 (1994).
4. E. Vives, P. Brodin, and B. Lebleu. A truncated HIV-1 Tat protein basic domain rapidly translocates through the plasma membrane and accumulates in the cell nucleus. *J. Biol. Chem.* **272**:16010–16017 (1997).
5. S. Futaki. Arginine-rich peptides: potential for intracellular delivery of macromolecules and the mystery of the translocation mechanisms. *Int. J. Pharm.* **245**:1–7 (2002).
6. R. Trehin, U. Krauss, A. G. Beck-Sickinger, H. P. Merkle, and H. M. Nielsen. Cellular uptake but low permeation of human calcitonin-derived cell penetrating peptides and Tat(47-57) through well-differentiated epithelial models. *Pharm. Res.* **21**:1248–1256 (2004).
7. R. Trehin, U. Krauss, R. Muff, M. Meinecke, A. G. Beck-Sickinger, and H. P. Merkle. Cellular internalization of human calcitonin derived peptides in MDCK monolayers: a comparative study with Tat(47-57) and penetratin(43-58). *Pharm. Res.* **21**:33–42 (2004).
8. A. Prochiantz. Getting hydrophilic compounds into cells: lessons from homeopeptides. *Curr. Opin. Neurobiol.* **6**:629–634 (1996).
9. S. R. Schwarze, A. Ho, A. Vocero-Akbani, and S. F. Dowdy. *In vivo* protein transduction: delivery of a biologically active protein into the mouse. *Science* **285**:1569–1572 (1999).
10. A. Astriab-Fisher, D. Sergueev, M. Fisher, B. R. Shaw, and R. L. Juliano. Conjugates of antisense oligonucleotides with the Tat and antennapedia cell-penetrating peptides: effects on cellular uptake, binding to target sequences, and biologic actions. *Pharm. Res.* **19**:744–754 (2002).
11. D. Singh, S. K. Bisland, K. Kawamura, and J. Gariepy. Peptide-based intracellular shuttle able to facilitate gene transfer in mammalian cells. *Bioconjug. Chem.* **10**:745–754 (1999).
12. M. Pooga, U. Soomets, M. Hallbrink, A. Valkna, K. Saar, K. Rezaei, U. Kahl, J. X. Hao, X. J. Xu, Z. Wiesenfeld-Hallin, T. Hokfelt, T. Bartfai, and U. Langel. Cell penetrating PNA constructs regulate galanin receptor levels and modify pain transmission *in vivo*. *Nat. Biotechnol.* **16**:857–861 (1998).
13. M. Lewin, N. Carlesso, C. H. Tung, X. W. Tang, D. Cory, D. T. Scadden, and R. Weissleder. Tat peptide-derivatized magnetic nanoparticles allow *in vivo* tracking and recovery of progenitor cells. *Nat. Biotechnol.* **18**:410–414 (2000).
14. U. Krauss, M. Muller, M. Stahl, and A. G. Beck-Sickinger. *In vitro* gene delivery by a novel human calcitonin (hCT)-derived carrier peptide. *Bioorg. Med. Chem. Lett.* **14**:51–54 (2004).
15. L. Crespo, G. Sanclimens, B. Montaner, R. Perez-Tomas, M. Royo, M. Pons, F. Albericio, and E. Giralt. Peptide dendrimers based on polyproline helices. *J. Am. Chem. Soc.* **124**:8876–8883 (2002).
16. J. Fernandez-Carneado, M. J. Kogan, S. Castel, and E. Giralt. Potential peptide carriers: amphipathic proline-rich peptides derived from the N-terminal domain of gamma-Zein. *Angew. Chem., Int. Ed. Engl.* **43**:1811–1814 (2004).
17. J. Fernandez-Carneado, M. J. Kogan, S. Pujals, and E. Giralt. Amphipathic peptides and drug delivery. *Biopolymers* **76**:196–203 (2004).
18. C. Foerg, U. Ziegler, J. Fernandez-Carneado, E. Giralt, R. Rennert, A. G. Beck-Sickinger, and H. P. Merkle. Decoding the entry of two novel cell-penetrating peptides in HeLa cells: lipid raft-mediated endocytosis and endosomal escape. *Biochemistry* **44**:72–81 (2005).
19. A. Ferrari, V. Pellegrini, C. Arcangeli, A. Fittipaldi, M. Giacca, and F. Beltram. Caveolae-mediated internalization of extracellular HIV-1 tat fusion proteins visualized in real time. *Mol. Ther.* **8**:284–294 (2003).
20. R. Fischer, K. Kohler, M. Fotin-Mleczek, and R. Brock. A stepwise dissection of the intracellular fate of cationic cell-penetrating peptides. *J. Biol. Chem.* **279**:12625–12635 (2004).
21. M. Hallbrink, A. Floren, A. Elmquist, M. Pooga, T. Bartfai, and U. Langel. Cargo delivery kinetics of cell-penetrating peptides. *Biochim. Biophys. Acta* **1515**:101–109 (2001).
22. M. Tyagi, M. Rusnati, M. Presta, and M. Giacca. Internalization of HIV-1 tat requires cell surface heparan sulfate proteoglycans. *J. Biol. Chem.* **276**:3254–3261 (2001).
23. S. Violini, V. Sharma, J. L. Prior, M. Dyszlewski, and D. Piwnica-Worms. Evidence for a plasma membrane-mediated permeability barrier to Tat basic domain in well-differentiated epithelial cells: lack of correlation with heparan sulfate. *Biochemistry* **41**:12652–12661 (2002).
24. X. Zhang, L. Wan, S. Pooyan, Y. Su, C. R. Gardner, M. J. Leibowitz, S. Stein, and P. J. Sinko. Quantitative assessment of the cell penetrating properties of RI-Tat-9: evidence for a cell type-specific barrier at the plasma membrane of epithelial cells. *Mol. Pharm.* **1**:145–155 (2004).
25. M. J. Cho, D. P. Thompson, C. T. Cramer, T. J. Vidmar, and J. F. Scieszka. The Madin Darby canine kidney (MDCK) epithelial cell monolayer as a model cellular transport barrier. *Pharm. Res.* **6**:71–77 (1989).
26. B. Rothen-Rutishauser, S. D. Kramer, A. Braun, M. Gunthert, and H. Wunderli-Allenspach. MDCK cell cultures as an epithelial *in vitro* model: cytoskeleton and tight junctions as indicators for the definition of age-related stages by confocal microscopy. *Pharm. Res.* **15**:964–971 (1998).
27. K. Simons and S. D. Fuller. Cell surface polarity in epithelia. *Annu. Rev. Cell Biol.* **1**:243–288 (1985).
28. J. Balcarova-Stander, S. E. Pfeiffer, S. D. Fuller, and K. Simons. Development of cell surface polarity in the epithelial Madin-Darby canine kidney (MDCK) cell line. *EMBO J.* **3**:2687–2694 (1984).
29. N. S. Harhaj and D. A. Antonetti. Regulation of tight junctions and loss of barrier function in pathophysiology. *Int. J. Biochem. Cell Biol.* **36**:1206–1237 (2004).
30. G. van Meer, B. Gumbiner, and K. Simons. The tight junction does not allow lipid molecules to diffuse from one epithelial cell to the next. *Nature* **322**:639–641 (1986).
31. G. van Meer and K. Simons. The function of tight junctions in maintaining differences in lipid composition between the apical and the basolateral cell surface domains of MDCK cells. *EMBO J.* **5**:1455–1464 (1986).
32. M. Cereijido, E. Robbins, D. D. Sabatini, and E. Stefani. Cell-to-cell communication in monolayers of epithelioid cells (MDCK) as a function of the age of the monolayer. *J. Membr. Biol.* **81**:41–48 (1984).
33. M. Cereijido, J. Valdes, L. Shoshani, and R. G. Contreras. Role of tight junctions in establishing and maintaining cell polarity. *Annu. Rev. Physiol.* **60**:161–177 (1998).
34. M. Hallbrink, J. Oehlke, G. Papsdorf, and M. Bienert. Uptake of cell-penetrating peptides is dependent on peptide-to-cell ratio rather than on peptide concentration. *Biochim. Biophys. Acta* **1667**:222–228 (2004).
35. H. R. Bourne. GTPases. A turn-on and a surprise. *Nature* **366**:628–629 (1993).
36. S. Etienne-Manneville and A. Hall. Rho GTPases in cell biology. *Nature* **420**:629–635 (2002).
37. M. Fukata, M. Nakagawa, and K. Kaibuchi. Roles of Rho-family GTPases in cell polarisation and directional migration. *Curr. Opin. Cell Biol.* **15**:590–597 (2003).
38. A. Hall. Rho GTPases and the actin cytoskeleton. *Science* **279**:509–514 (1998).
39. C. D. Nobes and A. Hall. Rho, rac, and cdc42 GTPases regulate the assembly of multimolecular focal complexes associated with actin stress fibers, lamellipodia, and filopodia. *Cell* **81**:53–62 (1995).
40. F. Rivero and B. P. Somesh. Signal transduction pathways regulated by Rho GTPases in Dictyostelium. *J. Muscle Res. Cell Motil.* **23**:737–749 (2002).
41. M. Symons and N. Rusk. Control of vesicular trafficking by Rho GTPases. *Curr. Biol.* **13**:R409–R418 (2003).
42. L. Van Aelst and C. D'Souza-Schorey. Rho GTPases and signaling networks. *Genes Dev.* **11**:2295–2322 (1997).
43. B. Qualmann, M. M. Kessels, and R. B. Kelly. Molecular links

between endocytosis and the actin cytoskeleton. *J. Cell Biol.* **150**:F111–F116 (2000).
44. B. Qualmann and H. Mellor. Regulation of endocytic traffic by Rho GTPases. *Biochem. J.* **371**:233–241 (2003).
45. A. M. Hopkins, S. V. Walsh, P. Verkade, P. Boquet, and A. Nusrat. Constitutive activation of Rho proteins by CNF-1 influences tight junction structure and epithelial barrier function. *J. Cell Sci.* **116**:725–742 (2003).
46. R. C. Orlando. Mechanisms of epithelial injury and inflammation in gastrointestinal diseases. *Rev. Gastroenterol. Disord.* **2**(Suppl 2):S2–S8 (2002).
47. D. S. Sanders. Mucosal integrity and barrier function in the pathogenesis of early lesions in Crohn's disease. *J. Clin. Pathol.* **58**:568–572 (2005).
48. H. Schmitz, C. Barmeyer, A. H. Gitter, F. Wullstein, C. J. Bentzel, M. Fromm, E. O. Riecken, and J. D. Schulzke. Epithelial barrier and transport function of the colon in ulcerative colitis. *Ann. N.Y. Acad. Sci.* **915**:312–326 (2000).
49. H. Schmitz, M. Fromm, C. J. Bentzel, P. Scholz, K. Detjen, J. Mankertz, H. Bode, H. J. Epple, E. O. Riecken, and J. D. Schulzke. Tumor necrosis factor-alpha (TNFalpha) regulates the epithelial barrier in the human intestinal cell line HT-29/B6. *J. Cell Sci.* **112**(Pt 1):137–146 (1999).
50. D. Siccardi, J. R. Turner, and R. J. Mrsny. Regulation of intestinal epithelial function: a link between opportunities for macromolecular drug delivery and inflammatory bowel disease. *Adv. Drug Deliv. Rev.* **57**:219–235 (2005).
51. C. B. Coyne, M. K. Vanhook, T. M. Gambling, J. L. Carson, R. C. Boucher, and L. G. Johnson. Regulation of airway tight junctions by proinflammatory cytokines. *Mol. Biol. Cell* **13**:3218–3234 (2002).
52. A. Trautmann, K. Kruger, M. Akdis, D. Muller-Wening, A. Akkaya, E. B. Brocker, K. Blaser, and C. A. Akdis. Apoptosis and loss of adhesion of bronchial epithelial cells in asthma. *Int. Arch. Allergy Immunol.* **138**:142–150 (2005).
53. P. Wunderbaldinger, L. Josephson, and R. Weissleder. Tat peptide directs enhanced clearance and hepatic permeability of magnetic nanoparticles. *Bioconjug. Chem.* **13**:264–268 (2002).
54. D. G. Hemmings, B. Lowen, R. Sherburne, G. Sawicki, and L. J. Guilbert. Villous trophoblasts cultured on semi-permeable membranes form an effective barrier to the passage of high and low molecular weight particles. *Placenta* **22**:70–79 (2001).
55. D. A. Mann and A. D. Frankel. Endocytosis and targeting of exogenous HIV-1 Tat protein. *EMBO J.* **10**:1733–1739 (1991).
56. T. Letoha, S. Gaal, C. Somlai, A. Czajlik, A. Perczel, and B. Penke. Membrane translocation of penetratin and its derivatives in different cell lines. *J. Mol. Recognit.* **16**:272–279 (2003).
57. C. Lamaze, A. Dujeancourt, T. Baba, C. G. Lo, A. Benmerah, and A. Dautry-Varsat. Interleukin 2 receptors and detergent-resistant membrane domains define a clathrin-independent endocytic pathway. *Mol. Cell* **7**:661–671 (2001).
58. B. J. Nichols, A. K. Kenworthy, R. S. Polishchuk, R. Lodge, T. H. Roberts, K. Hirschberg, R. D. Phair, and J. Lippincott-Schwartz. Rapid cycling of lipid raft markers between the cell surface and Golgi complex. *J. Cell Biol.* **153**:529–541 (2001).
59. P. A. Orlandi and P. H. Fishman. Filipin-dependent inhibition of cholera toxin: evidence for toxin internalization and activation through caveolae-like domains. *J. Cell Biol.* **141**:905–915 (1998).
60. V. Puri, R. Watanabe, R. D. Singh, M. Dominguez, J. C. Brown, C. L. Wheatley, D. L. Marks, and R. E. Pagano. Clathrin-dependent and -independent internalization of plasma membrane sphingolipids initiates two Golgi targeting pathways. *J. Cell Biol.* **154**:535–547 (2001).
61. G. Karp. *Cell and Molecular Biology*. John Wiley & Sons, Inc., 1999.
62. L. Pelkmans and A. Helenius. Endocytosis via caveolae. *Traffic* **3**:311–320 (2002).
63. L. Pelkmans, J. Kartenbeck, and A. Helenius. Caveolar endocytosis of simian virus 40 reveals a new two-step vesicular-transport pathway to the ER. *Nat. Cell Biol.* **3**:473–483 (2001).
64. J. P. Richard, K. Melikov, E. Vives, C. Ramos, B. Verbeure, M. J. Gait, L. V. Chernomordik, and B. Lebleu. Cell-penetrating peptides. A reevaluation of the mechanism of cellular uptake. *J. Biol Chem.* **278**:585–590 (2003).
65. S. Ellis and H. Mellor. Regulation of endocytic traffic by rho family GTPases. *Trends Cell Biol.* **10**:85–88 (2000).
66. S. M. Fish, R. Proujansky, and W. W. Reenstra. Synergistic effects of interferon gamma and tumour necrosis factor alpha on T84 cell function. *Gut* **45**:191–198 (1999).
67. M. Bruewer, A. Luegering, T. Kucharzik, C. A. Parkos, J. L. Madara, A. M. Hopkins, and A. Nusrat. Proinflammatory cytokines disrupt epithelial barrier function by apoptosis-independent mechanisms. *J. Immunol.* **171**:6164–6172 (2003).
68. A. Nusrat, C. A. Parkos, P. Verkade, C. S. Foley, T. W. Liang, W. Innis-Whitehouse, K. K. Eastburn, and J. L. Madara. Tight junctions are membrane microdomains. *J. Cell Sci.* **113** (Pt 10):1771–1781 (2000).
69. T. S. Jou, S. M. Leung, L. M. Fung, W. G. Ruiz, W. J. Nelson, and G. Apodaca. Selective alterations in biosynthetic and endocytic protein traffic in Madin-Darby canine kidney epithelial cells expressing mutants of the small GTPase Rac1. *Mol. Biol. Cell* **11**:287–304 (2000).
70. S. M. Leung, R. Rojas, C. Maples, C. Flynn, W. G. Ruiz, T. S. Jou, and G. Apodaca. Modulation of endocytic traffic in polarized Madin-Darby canine kidney cells by the small GTPase RhoA. *Mol. Biol. Cell* **10**:4369–4384 (1999).
71. S. Kuroda, M. Fukata, K. Fujii, T. Nakamura, I. Izawa, and K. Kaibuchi. Regulation of cell-cell adhesion of MDCK cells by Cdc42 and Rac1 small GTPases. *Biochem. Biophys. Res. Commun.* **240**:430–435 (1997).
72. K. Takaishi, T. Sasaki, H. Kotani, H. Nishioka, and Y. Takai. Regulation of cell–cell adhesion by rac and rho small G proteins in MDCK cells. *J. Cell Biol.* **139**:1047–1059 (1997).
73. A. H. Gitter, K. Bendfeldt, J. D. Schulzke, and M. Fromm. Leaks in the epithelial barrier caused by spontaneous and TNF-alpha-induced single-cell apoptosis. *FASEB J.* **14**:1749–1753 (2000).
74. N. Gassler, C. Rohr, A. Schneider, J. Kartenbeck, A. Bach, N. Obermuller, H. F. Otto, and F. Autschbach. Inflammatory bowel disease is associated with changes of enterocytic junctions. *Am. J. Physiol.: Gastrointest. Liver Physiol.* **281**:G216–G228 (2001).
75. T. Kucharzik, S. V. Walsh, J. Chen, C. A. Parkos, and A. Nusrat. Neutrophil transmigration in inflammatory bowel disease is associated with differential expression of epithelial intercellular junction proteins. *Am. J. Pathol.* **159**:2001–2009 (2001).
76. T. L. Bonfield, M. W. Konstan, and M. Berger. Altered respiratory epithelial cell cytokine production in cystic fibrosis. *J. Allergy Clin. Immunol.* **104**:72–78 (1999).
77. M. Naumann, S. Wessler, C. Bartsch, B. Wieland, A. Covacci, R. Haas, and T. F. Meyer. Activation of activator protein 1 and stress response kinases in epithelial cells colonized by *Helicobacter pylori* encoding the cag pathogenicity island. *J. Biol. Chem.* **274**:31655–31662 (1999).
78. J. B. Rothbard, S. Garlington, Q. Lin, T. Kirschberg, E. Kreider, P. L. McGrane, P. A. Wender, and P. A. Khavari. Conjugation of arginine oligomers to cyclosporin A facilitates topical delivery and inhibition of inflammation. *Nat. Med.* **6**:1253–1257 (2000).
79. M. Bucci, J. P. Gratton, R. D. Rudic, L. Acevedo, F. Roviezzo, G. Cirino, and W. C. Sessa. *In vivo* delivery of the caveolin-1 scaffolding domain inhibits nitric oxide synthesis and reduces inflammation. *Nat. Med.* **6**:1362–1367 (2000).